

# A study on impedance functions and input motions of embedded foundations by a hybrid approach

I. Takahashi, K. Yoshida & S. Nakai  
Shimizu Corporation, Tokyo, Japan

**ABSTRACT :** In this paper, a hybrid approach, which combines effective properties of both the finite element method and the boundary element method, is presented to calculate impedance functions and input motions of embedded foundations considering surrounding backfill soil. First, the formulation of the employed hybrid method is presented briefly. Next, numerical results are presented in order to demonstrate the accuracy of the present method by comparing the impedance functions and the input motions with those of existing results. After verifying the validity of the present hybrid method, several numerical calculations are carried out to investigate the effects of the existence of backfill soil on the impedance functions and the input motions of the embedded foundations and the influence of incidence angles of input waves on the input motions.

## 1 INTRODUCTION

In the aseismic design of large scale structures, it is important to evaluate dynamic soil-structure interaction effects correctly. The soil-structure interaction effects are mainly characterized by impedance functions which represent the dynamic force-displacement relationship between the foundations and the supporting soil and input motions which represent the motions of the massless foundations subjected to seismic waves. A number of techniques for the calculation of impedance functions and input motions have been proposed by a number of researchers. Among them, the finite element method is one of the powerful approaches (see Nakai et al. (1986)). The main advantage of the finite element method is to be able to model complicated soil-structure interaction systems such as embedded foundations and foundations surrounded by backfill soil. From the computational limitations, however, the finite element method cannot simulate an infinite region completely. An artificial boundary is inevitably needed when the finite element method is employed. On the other hand, the boundary element method (see Dominguez (1978), Yoshida and Kawase (1986)) has the advantage in modeling the unbounded region if Green's functions satisfying the radiation condition are employed. Though it is not difficult to satisfy the radiation condition analytically, it is not easy for the Green's functions to represent the complicated geometry near the foundations.

In this paper, a hybrid approach (see Mita and Luco (1989), Yoshida et al. (1990)), which combines the effective properties of both the finite element method and the boundary element method, is presented to calculate the impedance functions and the input motions of embedded foundations considering the surrounding backfill soil. As shown in Fig.1, the complicated region near the

foundation is modeled by the finite elements and the layered half-space around the complicated region is modeled by the boundary elements. The formulation of the employed hybrid method is presented briefly. The accuracy of the present method is verified through the comparison of numerical results obtained by the other method, followed by the several numerical calculations to investigate the effects of the existence of the backfill soil and the influence of the incidence angles of input waves.

## 2 FORMULATION OF HYBRID METHOD

In this section, the hybrid approach, which combines the finite element method and the boundary element method, is formulated for the soil-structure interaction analysis in a frequency domain. The entire soil-structure system can be divided into two subsystems; a near field subsystem including the structure and a far field subsystem. The structure and near field subsystem is modeled by the finite elements and the far field subsystem is modeled by the boundary elements. The fundamental stiffness equation for the finite element region can be given as,

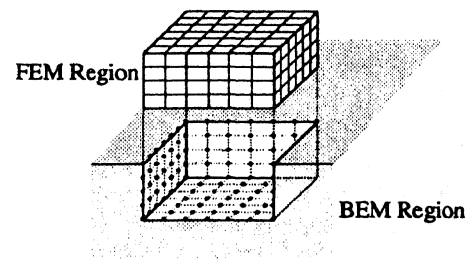


Fig.1 Model geometry

$$[K^F] \{u^F\} = \{f^F\} \quad (1)$$

where  $[K^F]$  is the dynamic stiffness matrix and  $\{f^F\}$  is the equivalent nodal force vector.  $\{u^F\}$  represents the displacement vector. The superscript  $F$  denotes the terms for the finite elements. On the other hand, the basic formulation of the boundary element method can be written as,

$$[c]^i \{u\}^i + \int_{\Gamma} [P^*] \{u\} d\Gamma - \int_{\Gamma} [U^*] \{p\} d\Gamma = \{u^f\}^i \quad (2)$$

where  $[c]^i$  is a constant matrix which is determined by the boundary configuration at a point  $i$ ,  $\{u\}^i$  is the displacement vector at that point,  $[U^*]$  and  $[P^*]$  are the displacement and the traction matrices respectively due to a unit point load at the point  $i$ .  $\{u\}$  and  $\{p\}$  are the boundary value vectors of the displacement and the traction, respectively.  $\Gamma$  is the integral domain and  $\{u^f\}^i$  is the vector for the analysis of wave impinging problems. In the present study, since the employed Green's functions satisfy the traction-free condition on the surface of the layered half-space (see Apsel (1979)), the integral domain  $\Gamma$  is only the interface between the finite element region and the boundary element region. By discretizing the integral domain into  $N$  elements, the integral equation (2) is transformed into the following form for each point  $i$  under consideration,

$$[c]^i \{u\}^i + \sum_{j=1}^N \left[ \int_{\Gamma} [P^*] [\Phi]^T d\Gamma \right] \{u\}_j - \sum_{j=1}^N \left[ \int_{\Gamma} [U^*] [\Phi]^T d\Gamma \right] \{p\}_j = \{u^f\}^i \quad (3)$$

where  $\{u\}_j$  and  $\{p\}_j$  are the displacement and the traction vectors of  $j$ -th element respectively, and  $[\Phi]^T$  is the interpolation function matrix. In this study, linear elements are used in the boundary element region to satisfy the compatibility condition with the finite element region. Finally the matrix equation for the boundary element region can be expressed as,

$$[H] \{u\} - [G] \{p\} = \{u^f\} \quad (4)$$

where  $[H]$  and  $[G]$  are the matrices which are constituted by Green's functions of the traction and displacement respectively. In order to combine the finite element region and the boundary element region, the equation (4) must be rearranged to a finite element form by inverting  $[G]$ . The final expression can be written as,

$$[K^B] \{u^B\} = \{f^B\} + \{f^{iB}\} \quad (5)$$

where  $[K^B]$  and  $\{u^B\}$  are the stiffness matrix and the nodal displacement vector for the boundary element region, respectively.  $\{f^B\}$  and  $\{f^{iB}\}$  are the nodal force vector and the equivalent nodal force vector caused by the impinging waves, respectively. The superscript  $B$  stands for the boundary element region. These terms are written as,

$$[K^B] = [D][G]^{-1}[H], \{f^B\} = [D]\{p\}, \{f^{iB}\} = [D][G]^{-1}\{u^i\} \quad (6)$$

where  $[D]$  represents the transformation matrix to convert the traction to the equivalent nodal force. On the interface between the finite elements and the boundary elements, the equilibrium and compatibility conditions must be satisfied as follows,

$$\{u_C^B\} = \{u_C^F\}, \{f_C^B\} + \{f_C^F\} = 0 \quad (7)$$

where the subscript  $C$  defines the interface. Finally the whole matrix equation can be given in the style used in the finite element method as follows,

$$\begin{bmatrix} K_{FF}^F & K_{FC}^F & 0 \\ K_{CF}^F & K_{CC}^F + K_{CC}^B & K_{CB}^B \\ 0 & K_{BC}^B & K_{BB}^B \end{bmatrix} \begin{Bmatrix} u_F \\ u_C \\ u_B \end{Bmatrix} = \begin{Bmatrix} f_F \\ f_C \\ f_B \end{Bmatrix} + \begin{Bmatrix} 0 \\ f_C^{iB} \\ f_B^{iB} \end{Bmatrix} \quad (8)$$

### 3 NUMERICAL RESULTS AND DISCUSSIONS

Numerical results are presented in order to demonstrate the accuracy of the present method by comparing the impedance functions and the input motions with those of existing results. An embedded foundation in an elastic half-space is chosen for comparison. Poisson's ratio of  $\nu=1/3$  is adopted throughout the analyses. After verifying the validity of the present hybrid method, several numerical calculations are carried out to investigate the effects of the existence of the backfill soil on the impedance functions and input motions of the embedded foundations, and the influence of incidence angles of input waves on the input motions.

#### 3.1 Verification of present method

The dynamic characteristics of a rigid foundation with  $2B \times 2B$  dimensions embedded in an elastic half-space to the depth of  $H=2B/3$  is analyzed. Figs. 2 and 3 show the analysis model and the coordinate system. The foundation is assumed to be perfectly bonded to the soil. This model consists of 228 finite elements and 220 surrounding boundary elements. The bottom of the rigid foundation is discretized into  $6 \times 6$  finite elements, while each side wall is covered by two elements. The material damping constant is taken to be 0.03 for the half-space.

In Fig. 4, the impedance functions of the embedded foundation are shown against the non-dimensional frequency  $a_0 (= \omega B / V_{sb})$ , where  $\omega$  is the circular frequency and  $V_{sb}$  is the shear wave velocity of the underlying half-space. The impedance functions are referred to the center of the bottom of the foundation and normalized by the shear modulus  $G_0$  of the half-space and the half width  $B$  of the foundation throughout the presentation of impedance functions. The results obtained by Mita and Luco (1989) using a hybrid method of the finite element method and the boundary integral equation method are also plotted in the figure. It can be concluded from this figure that the present hybrid method gives sufficiently accurate results of impedance functions compared with those obtained by Mita and Luco (1989). Some difference in the imaginary

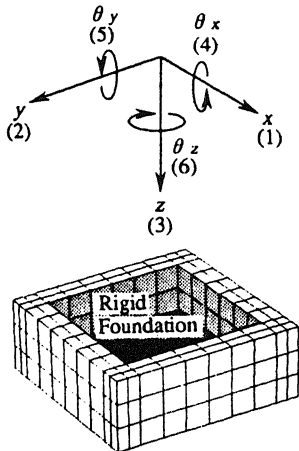


Fig. 2 Mesh layout and coordinate system

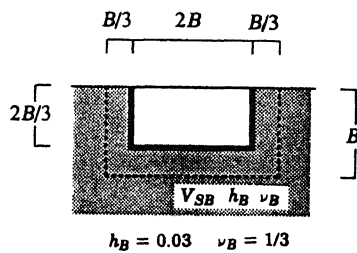


Fig. 3 Description of embedded foundation

part of the impedance functions may arise from the fact that the material damping constant is taken to be 0.03 for the half-space in this study while the material damping is not considered in the analyses by Mita and Luco (1989).

Fig. 5 shows the input motions when the foundation is subjected to a vertically incident SH wave and Fig. 6 shows the input motions when subjected to a horizontally incident SH wave against the non-dimensional frequency  $a_0$ . The rocking and torsional motions are evaluated from the vertical and horizontal motions at the edge of the foundation respectively. The input motions are referred to the center of the bottom of the foundation and normalized by free-field surface ground motions throughout the presentation of input motions. The results by the present method agree well with those obtained by Mita and Luco (1989) for both vertically and horizontally incident SH waves.

The present hybrid method is verified through the comparison of the impedance functions and the input motions with those of the existing results.

### 3.2 Effects of backfill soil

In order to investigate the effects of the backfill soil on the

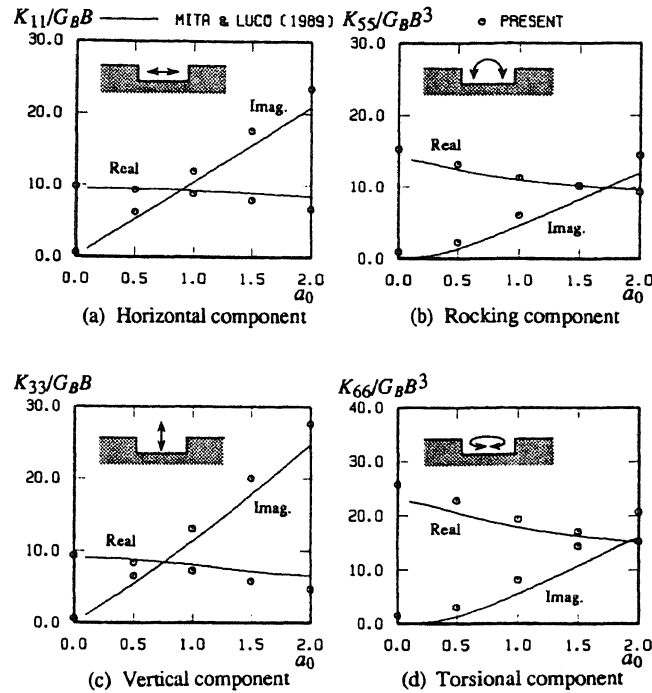


Fig. 4 Impedance functions of embedded foundation in elastic half-space

impedance functions and the input motions of an embedded foundation, four surrounding soil models are considered as shown in Fig. 7. The first soil model is an elastic half-space, the second one is an elastic half-space with a backfill soil on the sides of a foundation, the third one is an elastic half-space with a backfill soil on the sides and at the bottom of a foundation, and the last one is a two layered half-space. The width of the backfill soil is set to be  $B/3$ . The physical properties of the backfill soil are assumed to be the same as those of the surface layer of the two layered model. The discretization of the foundation and the surrounding soil is shown in Fig. 2 and the foundation embedment of  $H=2B/3$  are common to the four models.

Fig. 8 shows the normalized impedance functions of the embedded foundations for the four surrounding soil models against the non-dimensional frequency  $a_0$ . From this figure, it is clear that the effects of the backfill soil mainly appear in the imaginary part of the translational components of the impedance functions and in the real part of the rotational components. As for the real part of the horizontal impedance functions, the effect of the layer is more remarkable than that of the backfill soil, since the difference between the layered model and the backfill model is larger than that between the half-space model and the backfill model. On the other hand, the figure shows that the imaginary part of the horizontal impedance functions is mainly determined by the soil of the vicinity of the foundation. This comes from the fact that there exists little difference in the impedance functions between the two layered model and the model with the backfill on

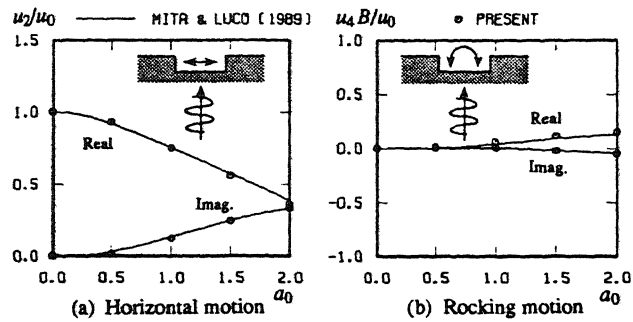


Fig.5 Input motions of embedded foundation due to vertically incident SH wave

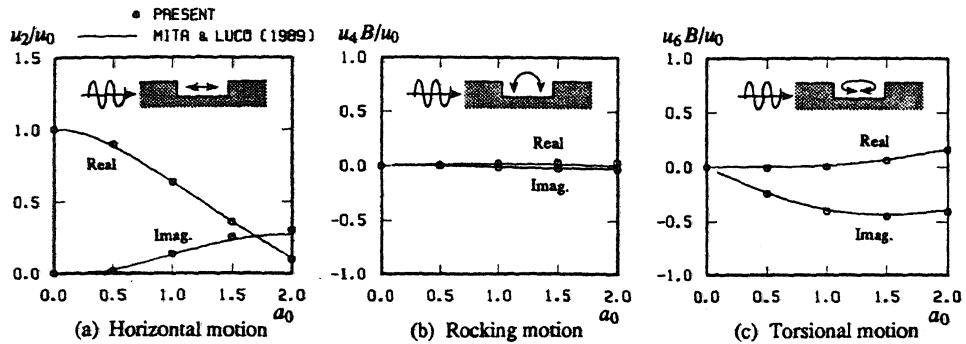


Fig.6 Input motions of embedded foundation due to horizontally incident SH wave

the sides and at the bottom. This tendency can be seen in the imaginary part of other components of the impedance functions. It should be noted that the real part of the vertical impedance functions is little affected with the existence of the layer or the backfill soil.

Fig. 9 shows the input motions of the embedded foundations for the four surrounding soil models when the foundations are subjected to vertically incident SH waves. It is clear from the comparison of the results that the existence of the backfill soil or the layer mainly affects the real part of horizontal motions. When the backfill soil exists only on the sides of the foundation, the real part of the horizontal motions decreases and the imaginary part increases slightly. The influence of the layer is more remarkable than that of the existence of the backfill soil only on the sides of the foundation, from the fact that the real part of the horizontal motions of the two layered model shows a fairly significant decrease and the imaginary part increases more than that of the half-space model. However, when the backfill soil exists partially both on the sides and at the bottom, the results have the different tendency from those of two layered model or the model with the backfill only on the sides of the foundation. As for the rotational motions, the influence of the backfill soil or the layer appears in a high frequency range.

### 3.3 Influence of incidence angles of input waves

In this section, the influence of incidence angles of input waves on the input motion is discussed. The input motions of the embedded foundation in an elastic half-space are analyzed when the foundation is subjected to obliquely incident SH and SV waves. The foundation embedment ratio  $H/B$  is  $2/3$  and the material damping constant of the elastic half space is assumed to be 0.03.

Fig. 10 shows the input motions of the foundation for a vertically incident SH wave and an obliquely incident SH wave at the angle of 20 degrees (see Fig. 7(a)). The torsional motions are produced mainly in the imaginary part due to the obliquely incident SH wave. In Fig. 11, the input motions of the foundation are shown for a vertically incident SV wave and an obliquely incident SV wave at the angle of 20 degrees. When the foundation is subjected to the obliquely incident SV wave, rocking motions increase mainly in the imaginary part. From the figures, it is clear that the rocking motions increase or torsional motions are produced due to the obliquely incident waves.

## 4 CONCLUSIONS

In this paper, the dynamic response characteristics of an embedded foundation are examined considering the backfill soil effects and the influence of incidence angles

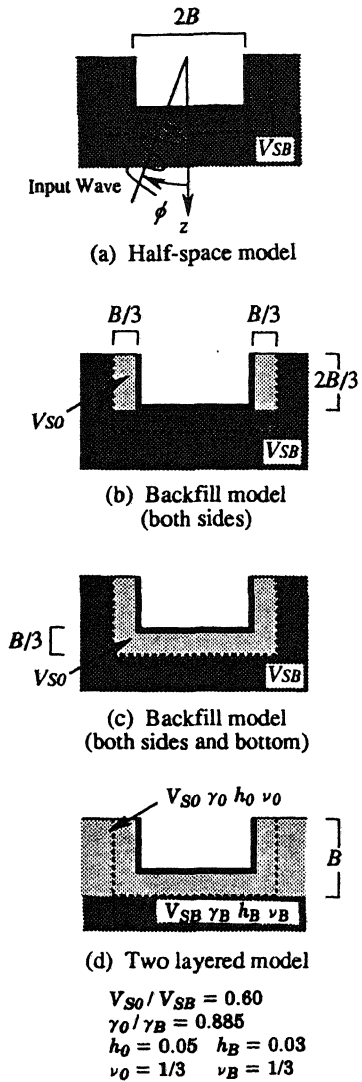


Fig. 7 Description of models

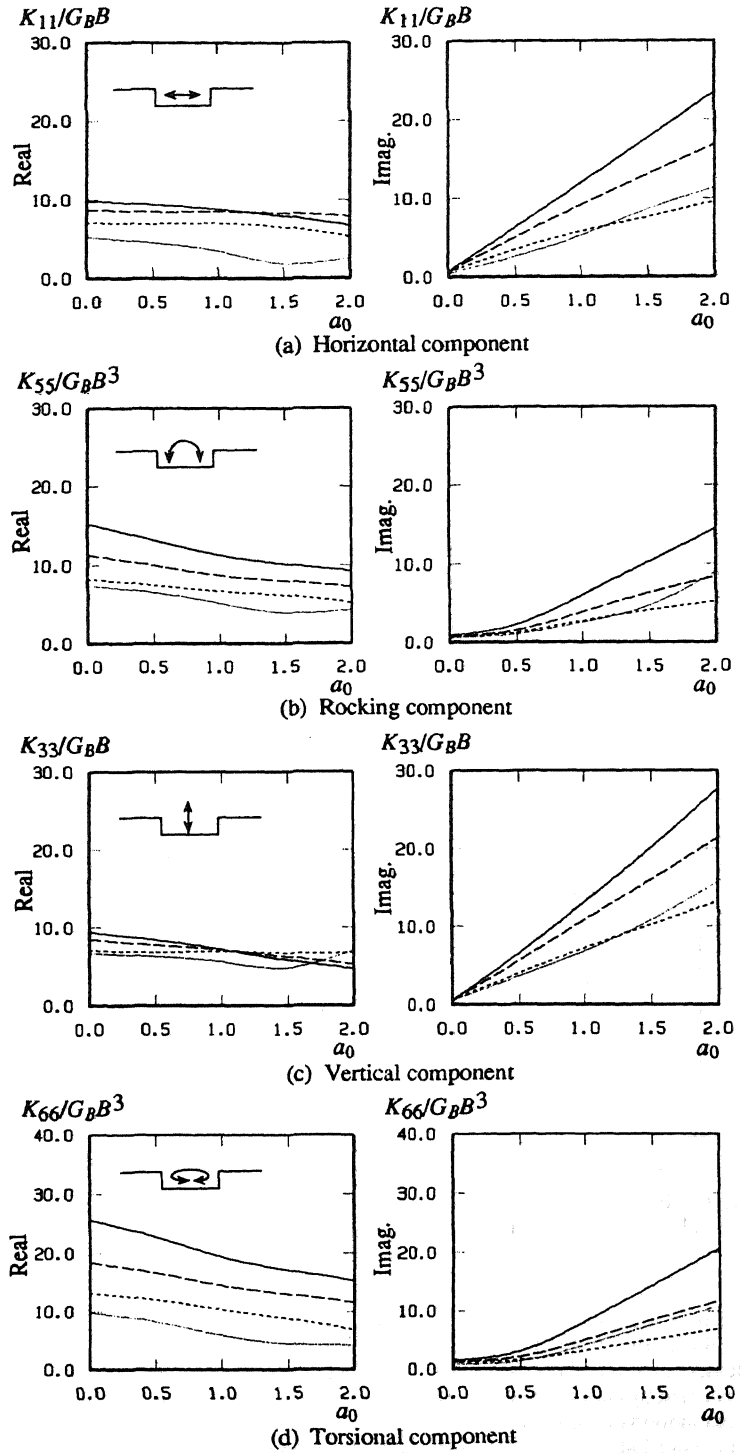
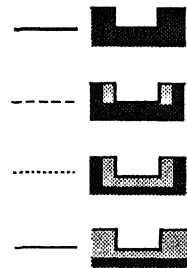


Fig. 8 Impedance functions of embedded foundations with backfill soil

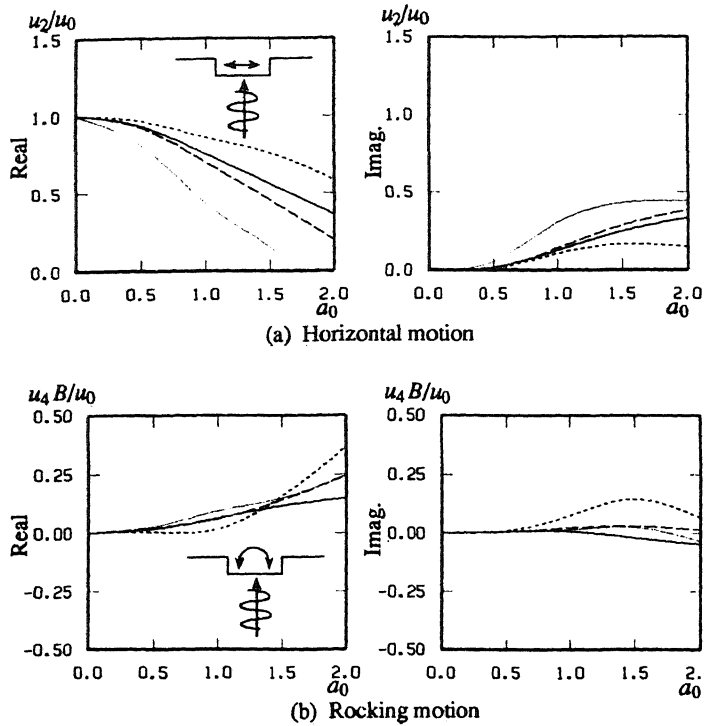


Fig. 9 Input motions of embedded foundations due to vertically incident SH wave

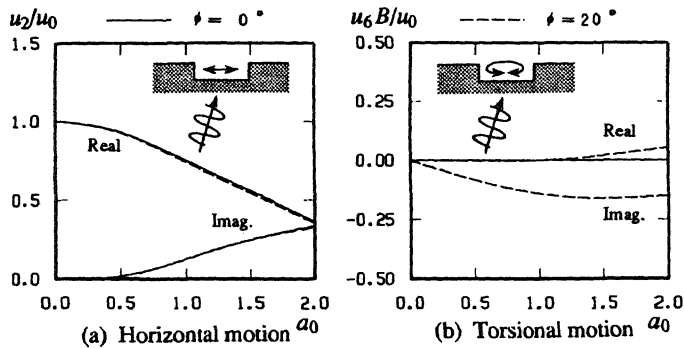


Fig. 10 Input motions of embedded foundation in elastic half-space due to vertically and obliquely incident SH waves

of input waves in the aid of a hybrid method which combines the finite element method and the boundary element method. The effectiveness of the present method is verified by comparing the impedance functions and the input motions with those of existing numerical solutions. It is found that the backfill soil effects mainly appear in the imaginary part of the translational impedance functions and in the real part of the rotational impedance functions. The influence of the backfill soil or the layer mainly appear in the real part of horizontal input motions.

#### ACKNOWLEDGEMENT

The authors would like to express their appreciation to Prof. Luco of the University of California, San Diego for his helpful suggestions.

#### REFERENCES

Apse, R. J., "Dynamic Green's Functions for Layered

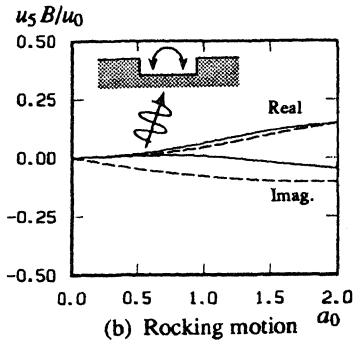
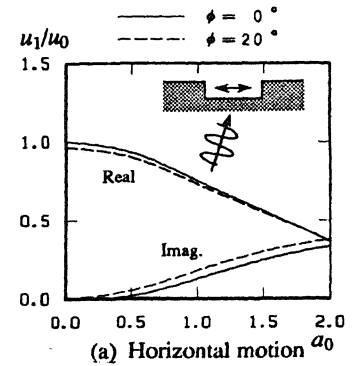
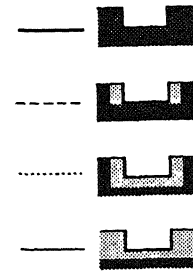


Fig. 11 Input motions of embedded foundation in elastic half-space due to vertically and obliquely incident SV waves

- Media and Applications to Boundary-value Problems," *Ph.D. Thesis*, UCSD, 1979
- Dominguez, J., "Dynamic Stiffness of Rectangular Foundations," *M.I.T. Research Report*, R78-20, 1978
- Mita, A. and Luco, J.E., "Impedance Functions and Input Motions for Embedded Square Foundations," *Journal of Geotechnical Engineering*, ASCE, vol.115, NO4, 1989
- Nakai, S. et al. "Simplified Infinite Boundary for Three-dimensional Finite Element Analysis of Soil-structure Interaction," *Proc. of 7th. Japan Earthquake Engineering Symposium*, 1986
- Yoshida, K. and Kawase, H., "Dynamic Cross-interaction of Embedded Foundations," *Proc. of 7th. Japan Earthquake Engineering Symposium*, 1986 (in Japanese)
- Yoshida, K. et al. "On the Dynamic Characteristics of Embedded Foundations Considering Backfill Effects by A Hybrid Approach," *Proc. of 8th. Japan Earthquake Engineering Symposium*, 1990